

Learning-Accelerated ADMM for Distributed Optimal Power Flow

Dave Biagioni, Peter Graf, Xiangyu Zhang, Jennifer King
National Renewable Energy Laboratory, Golden, CO, USA
{dave.biagioni, peter.graf, xiangyu.zhang, jennifer.king}@nrel.gov

Abstract—We propose a novel data-driven method to accelerate the convergence of Alternating Direction Method of Multipliers (ADMM) for solving distributed DC optimal power flow (DC-OPF) where lines are shared between independent network partitions. Using previous observations of ADMM trajectories for a given system under varying load, the method trains a recurrent neural network (RNN) to predict the converged values of dual and consensus variables. Given a new realization of system load, a small number of initial ADMM iterations is taken as input to infer the converged values and directly inject them into the iteration. For this purpose, we utilize a recently proposed RNN architecture called antisymmetric RNN (aRNN) that avoids vanishing and exploding gradients via network weights designed to have the spectral properties of a convergent numerical integration scheme. We demonstrate empirically that the online injection of these values into the ADMM iteration accelerates convergence by a factor of 2-50x for partitioned 13-, 300- and 2848-bus test systems under differing load scenarios. The proposed method has several advantages: it can be easily integrated around an existing software framework, requiring no changes to underlying physical models; it maintains the security of private decision variables inherent in consensus ADMM; inference is fast and so may be used in online settings; historical data is leveraged to improve performance instead of being discarded or ignored. While we focus on the ADMM formulation of distributed DC-OPF in this paper, the ideas presented are naturally extended to other iterative optimization schemes.

Index Terms—optimal power flow, recurrent neural network, alternating direction method of multipliers, machine learning, data-driven optimization

I. INTRODUCTION

The electric power grid is continually progressing towards a more complex, uncertain, and decentralized state. This fact stems from a variety of sources including higher penetration of renewable generation, increased presence of smart devices and subsystems, and market deregulation, to name a few. While this progression presents a number of operational and analytical challenges, the corresponding increase in available data paves the way for new approaches to improving system-wide efficiency and coordination.

This work was authored by the National Renewable Energy Laboratory, operated by Alliance for Sustainable Energy, LLC, for the U.S. Department of Energy (DOE) under Contract No. DE-AC36-08GO28308. Funding was provided by the Autonomous Energy Systems project funded by the National Renewable Energy Laboratory's Laboratory Directed Research and Development program. The views expressed in the article do not necessarily represent the views of the DOE or the U.S. Government. The U.S. Government retains and the publisher, by accepting the article for publication, acknowledges that the U.S. Government retains a nonexclusive, paid-up, irrevocable, worldwide license to publish or reproduce the published form of this work, or allow others to do so, for U.S. Government purposes.

In this paper, we consider the specific operational problem of direct current optimal power flow (DC-OPF) in which the network is decomposed into independently operating partitions. Because each partition is connected to others via one or more branches, agreement on these line flows is required as part of an optimal solution. While there are many possible ways to solve this *consensus* problem in a distributed fashion, we focus on the Alternating Direction Method of Multipliers (ADMM) due to its recent popularity for solving such problems [1], [2], [3], [4]. We note, however, that the ideas proposed in this paper are readily extensible to other iterative solution techniques.

In the spirit of several recent analyses of ADMM [5], [6], we view the iterations as the time steps of a discrete, stable dynamical system whose equilibria correspond to an optimal solution of the underlying optimization problem. The proposed method, which we call *learning-accelerated ADMM (LA-ADMM)*, aims to leverage previously observed trajectories as training data to build a machine learning (ML) model to predict the equilibrium values using only a small number of initial iterates. Once such a model is trained, optimal values can be inferred online and injected directly into the iteration to accelerate its convergence. For the prediction task, we propose the use of the antisymmetric recurrent neural network (aRNN) [7] and argue that this is a sound choice based on the theoretical properties of the network weights.

The use of ML in power systems is a growing area of research. Interest in distributed optimization algorithms themselves is also on the rise due to the increasing prevalence of physically distributed, autonomous systems and the frequent intractability of centralized formulations that assume complete knowledge of the system's state and dynamics. The optimal power flow problem, in particular, is amenable to the use of distributed methods as evidenced by several recent reviews [8], [9] and applications utilizing ADMM [10], [11], [12], [13], [14], [15], [16]. This paper sits at the intersection of these two research areas and specifically aims to augment the latter with the former.

Many straightforward applications of ML in OPF and related problems are either *centralized* in the sense that training requires a complete knowledge of the system's state and dynamics, or *intrusive* in the sense that target models are created *de novo* or to replace an existing one; see, e.g., [17], [18], [19] for recent examples. Our approach requires neither centralization nor intrusiveness. While it can leverage

centralized models to accelerate the training process, it only requires access to the consensus variables for training and inference. In addition, because predicted values are fed into the optimization models as iteration parameters, the method is distinctly non-intrusive.

The paper is organized as follows. In the remainder of this section, we briefly summarize the components of the proposed method, namely, the DC-OPF problem, its distributed formulation via ADMM, and the aRNN used for the prediction task. In section II we describe empirical experiments for three test systems and present the results of using standard ADMM versus LA-ADMM. Section III discusses further issues, conclusions and future work.

A. DC Optimal Power Flow Formulation

We briefly state the optimal power flow problem, referring the reader to several recent literature reviews for further details. The formulation we adopt utilizes branch flow variables in favor of voltage angles which, in our view, simplifies the notation for ADMM (cf. Section I-B) since the consensus is stated in terms of individual variables (flows) rather than the difference between variables (voltage angles).

The aim of the DC-OPF is to determine the least-cost dispatch of generation subject to network constraints and load. Using a DC approximation to the full power flow equations leads to the following optimization problem:¹

$$\min_{\mathbf{x}, \mathbf{y}} f(\mathbf{x}) \quad (2)$$

$$\text{s. t. } \mathbf{A}\mathbf{y} + \mathbf{x} - \mathbf{d} = \mathbf{0} \quad (3)$$

$$\underline{\mathbf{x}} \leq \mathbf{x} \leq \bar{\mathbf{x}}, \quad \underline{\mathbf{y}} \leq \mathbf{y} \leq \bar{\mathbf{y}}. \quad (4)$$

Here $\mathbf{x}, \mathbf{d} \in \mathbb{R}^m$ are the active power generation and load at each of m buses, respectively, and $\mathbf{y} \in \mathbb{R}^n$ is the current flow along each of n branches. Upper and lower bounds on \mathbf{x}, \mathbf{y} are denoted by $\bar{(\cdot)}, \underline{(\cdot)}$, respectively. $A \in \mathbb{R}^{m \times n}$ is a network incidence matrix with $A_{ij} = -1$ for flows “from i to j ”, $A_{ij} = +1$ “from j to i ”, and $A_{ij} = 0$ otherwise. The vector of all zeros, $\mathbf{0}$, has dimension determined by context (here, $\mathbf{0} \in \mathbb{R}^m$). The cost function $f : \mathbb{R}^m \rightarrow \mathbb{R}$ representing the cost of generation is assumed to be quadratic and separable, i.e., $f(\mathbf{x}) = \mathbf{x}^T \text{diag}(\mathbf{c})\mathbf{x}$ where $\mathbf{c} \geq \mathbf{0}$.

B. Distributed DC-OPF Formulation via ADMM

In the distributed DC-OPF problem, the network is partitioned physically and/or computationally into separate components that share some number of the optimization variables. In this paper, we specifically consider the partitioning of buses into P disjoint sets indexed by \mathcal{I}_p , such that $\cup_{p=1}^P \mathcal{I}_p =$

¹An alternative formulation of the DC-OPF, popular in the power systems literature, can be derived in terms of voltage angles rather than current flow via

$$\sum_{j=1}^n A_{ij} y_j = \sum_{k=1}^m (\theta_i - \theta_k) / X_{ik}, \quad i = 1, \dots, m, \quad (1)$$

by selecting a reference bus $\hat{i} \in \{1, \dots, m\}$ such that $\theta_{\hat{i}} = 0$, and updating the power balance (3) and flow limit constraints (4) accordingly. In (1), X is the $m \times m$ network reactance matrix.

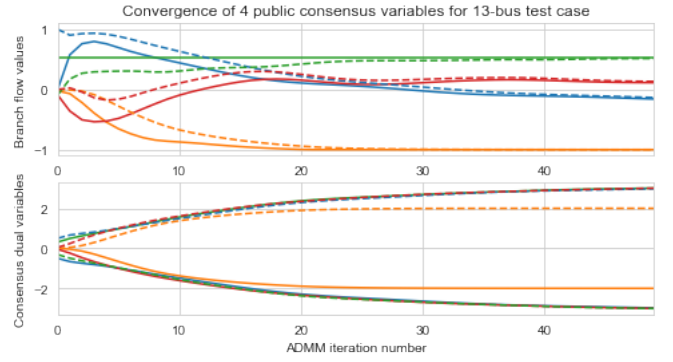


Fig. 1. Convergence of a consensus ADMM iteration for 4 of the 12 public variable pairs in the 13-bus test system. The remaining 8 variables pairs follow similar convergence patterns but are suppressed here for clarity. In this experiment, all 12 edges are public and thus each have a pair of primal and dual values corresponding to their “from” and “to” buses, denoted by solid and dashed lines, respectively. As the iteration approaches an optimal solution, the primal variables approach consensus while dual variables agree up to opposite sign. This image illustrates the viewpoint of ADMM as a discrete dynamical system approaching a steady state at optimality.

$\{1, \dots, m\}$ and $\mathcal{I}_p \cap \mathcal{I}_q = \delta(p, q)$. In other words, a bus i belongs to partition p if and only if $i \in \mathcal{I}_p$. Such a partitioning naturally leads to branch partitions whose index sets we denote as \mathcal{J}_{pq} , where p, q refer to the indexes of the adjacent partitions. We use the terminology of *public* versus *private* to distinguish between decision variables that are shared between partitions and internal to a partition, respectively. Using the above notation, we note that public variables consist only of branches with indices in \mathcal{I}_{pq} where $p \neq q$, and denote the size of this set by n_{pub} . In contrast, all bus-level decisions indexed by \mathcal{I}_q and internal branches indexed by \mathcal{J}_{pp} are private decision variables. The number of private decision variables is thus $m + n_{pri}$ where $n_{pri} = n - n_{pub}$. Finally, we use subscript p to denote partition membership of bus-level decisions and pq for branch-level decisions.

The global DC-OPF problem (2)-(4) can be expressed in terms of the partitions by

$$\min_{\mathbf{x}, \mathbf{y}} \sum_{p=1}^P f_p(\mathbf{x}_p) \quad (5)$$

$$\text{s. t. } A_{pq} \mathbf{y}_{pq} + \mathbf{x}_p - \mathbf{d}_p = \mathbf{0}_p, \quad \forall p \quad (6)$$

$$\underline{\mathbf{x}}_p \leq \mathbf{x}_p \leq \bar{\mathbf{x}}_p, \quad \underline{\mathbf{y}}_p \leq \mathbf{y}_p \leq \bar{\mathbf{y}}_p, \quad \forall p \quad (7)$$

where A_{pq} denotes the sub-blocks of the global incidence matrix A for all buses $i \in \mathcal{I}_q$ and branches $j \in \mathcal{J}_{pq}$ for $q = 1, \dots, P$. In other words, the constraint enforces power balance on all internal nodes subject to both internal and shared flows. The partition-wise cost functions f_p are defined to be 0 for all arguments $x_q, q \neq p$ and $f_p(x_p)$ otherwise.

Were it not for the public flow variables \mathbf{y}_{pq} , the above problem (5)-(7) could be trivially decomposed into P disjoint problems whose independent solution yields the global minimum. In the presence of these variables, however, decomposition requires additional constraints that enforce consensus. ADMM accomplishes this task via an augmented Lagrangian

formulation (see the classic reference [2] for more details) that drives local copies of public variables into consensus with the partitions that share them. Algorithmically, consensus ADMM equates to the following iterative scheme consisting of P independent primal optimizations followed by a centralized dual update,

$$\mathbf{y}_{pq}^{k+1} = \underset{\mathbf{x}_p, \mathbf{y}_{pq} \in \mathcal{X}_p}{\operatorname{argmin}} f_p(\mathbf{x}_p) + \boldsymbol{\lambda}_{pq}^{k,T} (\mathbf{y}_{pq} - \bar{\mathbf{y}}_{pq}^k) + \frac{\rho}{2} \|\mathbf{y}_{pq} - \bar{\mathbf{y}}_{pq}^k\|_2^2 \quad (8)$$

$$\bar{\mathbf{y}}_{pq}^{k+1} = \frac{1}{2} (\mathbf{y}_{pq}^k + \mathbf{y}_{qp}^k) \quad (9)$$

$$\boldsymbol{\lambda}_{pq}^{k+1} = \boldsymbol{\lambda}_{pq}^k + \rho (\mathbf{y}_{pq}^{k+1} - \bar{\mathbf{y}}_{pq}^{k+1}). \quad (10)$$

where we have introduced Lagrange multipliers $\boldsymbol{\lambda}_{pq} \in \mathbb{R}^{|\mathcal{J}_{pq}|}$ and used \mathcal{X}_p to denote the local constraint set for partition p .

C. Antisymmetric Recurrent Neural Networks

As mentioned briefly in Section I, one way to view the ADMM iteration is as a numerical integration scheme for solving the dynamical system

$$\frac{d}{dt} u(t) = -\nabla f(u(t)). \quad (11)$$

Note that steady states of this system coincide with local optima of f since $du/dt = 0 \iff \nabla f = 0$. This point of view has proven useful in several recent works analyzing the convergence and designing accelerated variants of ADMM [5], [6]. It is also empirically intuitive; see, e.g., Fig. 1 showing convergence of a subset of ADMM variables for the 13-bus system described in Section II.

In this paper, we adopt the dynamical systems point of view of ADMM and select a machine learning algorithm with suitable properties. The recently proposed aRNN is particularly suitable because, unlike many other RNN variants, it is explicitly designed to have spectral properties like those of a stable numerical integration scheme. The network architecture is given by

$$\mathbf{z}_t = \sigma(U_h(\gamma)\mathbf{h}_{t-1} + V_z\mathbf{x}_t + \mathbf{b}_z) \quad (12)$$

$$\mathbf{h}_t = \mathbf{h}_{t-1} + \epsilon \mathbf{z}_t \circ \tanh(U_h(\gamma)\mathbf{h}_{t-1} + V_h\mathbf{x}_t + \mathbf{b}_h) \quad (13)$$

where $U_h(\gamma) \equiv W_h - W_h^T - \gamma I$, $\gamma, \epsilon > 0$ are scalar hyperparameters, and \circ indicates elementwise multiplication. The vectors $\mathbf{x}_t, \mathbf{h}_t, \mathbf{z}_t$ are the network inputs, recurrent inputs, and gate activations at time t , respectively. W_h is an upper diagonal, trainable weight matrix that gets applied in the recurrence (to the RNN hidden state). The remaining weights $V_{(\cdot)}, \mathbf{b}_{(\cdot)}$ are trainable network weights and biases, respectively. Crucially, the matrix U_h used in the recurrent layer has negative real eigenvalues by design and thus stabilizes the network output. This fact, combined with lower parameter complexity for comparable state-of-the-art RNNs, (2-3x fewer weights, see [7]), make aRNN an attractive choice for the ADMM prediction task.

TABLE I

TEST SYSTEMS. NOTATION: m DENOTES THE NUMBER OF BUSES, n THE NUMBER OF BRANCHES, n_{pub} THE NUMBER OF PUBLIC BRANCHES SPANNING P PARTITIONS, ρ THE ADMM STEP SIZE. THE VALUE OF ρ FOR THE 13-BUS SYSTEM WAS INTENTIONALLY CHOSEN TO ELICIT SLOW ADMM CONVERGENCE, TO DEMONSTRATE THAT ACCELERATION IS POSSIBLE EVEN IN THIS CASE.

Name	m	n	n_{pub}	P	ρ
IEEE 13	13	12	12	13	1
IEEE 300	300	411	24	5	1000
RTE 2848	2848	3776	231	20	1000

II. METHODS AND RESULTS

A. Methods

1) *Test systems*: The three test systems we considered were the IEEE 13-bus, IEEE 300-bus, and RTE 2848-bus systems. The 13-bus system served as exemplar for a system that is fully decomposed ($P = 13$, i.e., one node per partition) and was populated with fictitious data. Data for the two larger systems were obtained via the open source Power Grid Lib (*pglib*) repository [20]. Network properties were obtained directly from the repository, while load data was used to seed the training, as described in the following paragraph.

2) *Simulation of load*: A central tenet of our approach is to “learn to optimize from an abundance of data.” To this end, we identified three target systems with corresponding marginal costs of generation as well as generator and line limits. Keeping network properties fixed, we sampled many instances of system load and solved the resulting DC-OPF problem to obtain optimal values of both primal and dual variables. While we envision optimal values coming from converged ADMM iterations in any real-world scenario, it is also possible to accelerate training on simulated systems by running ADMM for a small number of iterations to gather what will be the input for the aRNN and then using a centralized solution to extract prediction targets (i.e. converged Lagrange multipliers and consensus variables). We used the latter approach, running ADMM for no more than 10 iterations to obtain training inputs and using the centralized solution for prediction targets. Load for all three systems was sampled according to the following strategy. We first defined a characteristic load for each bus, \bar{d}_i , from existing *pglib* data for the 300- and 2848-bus systems and randomly for the 13-bus system. We then generated load scenarios for each bus,

$$d_i(\chi, \xi_i) = \chi(1 + \xi_i)\bar{d}_i, \quad \chi, \xi_i \in U(0, 1), \quad \forall i \quad (14)$$

where $U(0, 1)$ denotes the uniform distribution on $(0, 1)$. Note that the variables χ is a system-wide scaling factor while ξ_i scales only the load at bus i . The net result is a profile that is between 0 – 200% of the nominal value both in terms of bus-level and total load.

3) *Network partitioning*: Partitioning of the network was performed using a Fluid Communities detection algorithm proposed in [21], with the resulting number of cuts and partitions summarized in Table I. This algorithm was chosen for this study because it is fast, simple to use, and leads to qualitatively

TABLE II

SUMMARY OF RESULTS. SYMBOLS μ_K AND σ_K ARE THE MEAN AND STANDARD DEVIATION FOR THE NUMBER OF ITERATIONS TO CONVERGENCE ACROSS THE INDICATED NUMBER OF TEST SAMPLES. THE RATIO COLUMN SHOWS THE TOTAL RATIO OF RUNS THAT CONVERGED IN THE ALLOTTED 50 ITERATIONS. CONVERGENCE TOLERANCE WAS 10^{-3} .

System Name	Test Samples	ADMM		LA-ADMM	
		$\mu_K \pm \sigma_K$	ratio	$\mu_K \pm \sigma_K$	ratio
IEEE 13	1000	$50 \pm 0^*$	0.000	14.3 ± 8.0	0.996
IEEE 300	992	37.4 ± 10.0	0.672	18.6 ± 9.5	0.958
RTE 2848	376	48.2 ± 2.2	0.523	10.2 ± 3.6	1.000

* ADMM did not converge to specified accuracy for any samples.

reasonable partitions. Partitioning can of course be performed in any number of ways depending on whether the goal is to, e.g., model real-world connectivity, or improve computational efficiency. However, these specific issues remain outside the scope of this paper.

4) *Training and Evaluation*: Typical best practices for model selection include cross validation, hyperparameter grid search, and regularization, to name a few. After extensive experimentation along these training dimensions, we adopted an approach that favored simplicity over accuracy with respect to a held-out test set. In particular, we identified a global set of hyperparameters and applied them to the aRNN trained for each test system. While this may lead to slightly suboptimal test set accuracy for any particular system, the approach is compelling in terms of ease of use and consistent, significant speed-up of ADMM. The most salient of the global hyperparameter values used were an aRNN layer size of 128, $\epsilon = 0.1$, and $\gamma = 10^{-4}$. We also found that using just $K = 4$ ADMM iterations for training led to a good balance of data efficiency and prediction accuracy. Optimization of the network weights was performed with respect to mean squared error on a held-out validation set using the stochastic gradient descent (“Adam” optimizer with a learning rate of 10^{-3}) and stopped after 10 iterations of stagnation in the validation loss or after 150 epochs, whichever was first.

The training set itself consisted of all public primal and dual variables for the first $K = 4$ iterations of ADMM as inputs, and converged consensus values as targets,

$$\text{Inputs : } (\lambda_{pq}^k, \bar{y}_{pq}^k, \mathcal{Y}_{pq}^k, \mathcal{Y}_{qp}^k) \in \mathbb{R}^{4n_{pub}}, \quad k = 1, \dots, K, \quad (15)$$

$$\text{Targets : } (\lambda_{pq}^*, \bar{y}_{pq}^*) \in \mathbb{R}^{2n_{pub}}. \quad (16)$$

Recall that $\bar{y}_{pq}^k = \bar{y}_{qp}^k$ and $\lambda_{pq}^k = -\lambda_{qp}^k$ by definition and so the second of each pair may be omitted from the training set.

To evaluate performance, new realizations of load were generated using the same procedure summarized in (14) and ADMM was run twice per sample: once, uninterrupted, for $K \gg 4$ iterations to provide a baseline, and a second time with aRNN predictions substituted for the current ADMM iterate at step $k = 4$, after which the λ 's and \bar{y} 's continue to evolve. The total number of steps to convergence and associated accuracies were then compared.

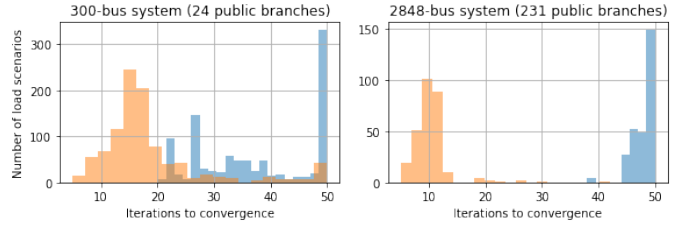


Fig. 2. Distribution of iterations to convergence with (light/orange) and without (dark/blue) injecting learned λ, \bar{y} values for the 300-bus and 2848-bus systems. Each iteration was stopped after 50 steps, meaning the right-most bins correspond to scenarios that did not converge in the allotted budget. For the 13-bus test case (not shown), none of the 1000 samples of standard ADMM converged within 50 iterations, while LA-ADMM converged in 14 ± 8 iterations on average (mean ± 1 -std).

B. Results

Results from applying the proposed method to the target problems are summarized in Figures 2-3 and Table II using a convergence threshold of 10^{-3} for both primal and dual residuals. All experiments were capped at 50 iterations. As indicated in Table II, none of the 1000 test samples converged for the 13-bus test case. This was by design (via a poor choice of ρ) to demonstrate that LA-ADMM could still perform well when using data from slowly converging iterations. Standard ADMM is able to converge for the 300- and 2848-bus test systems in at least half of the test problems, but it is still dramatically slower than with LA-ADMM.

A more detailed picture of convergence for these systems is shown in Figure 2, which shows the distributions of steps-to-convergence with and without learning. Yet another view for the 300-bus system is given in Figure 3 showing the progression of the dual and primal residuals as a function of iteration number. Here it is possible to see the exact point at which predictions are injected and the immediate effect on the residual values. In both subplots of Figure 3, the plateau in LA-ADMM beyond 20-25 iterations is somewhat devoid of information; comparing again with Figure 2, we see that most of the iterations have already converged by this number of steps.

III. DISCUSSION, CONCLUSION AND FUTURE WORK

While not necessary apparent today, the use of distributed optimization techniques such as ADMM will almost certainly be critical in future power systems operation. However, such decomposition comes with the drawback of the need to “iterate to self-consistency”. Our approach avoids this apparent jam by “pre-optimizing”; while there really is no free lunch, so we must do the work somewhere, by using computational cycles in an off-line learning mode we allow the online optimization for general inputs to be drastically sped up.

Generalizability: One may wonder not only whether our method generalizes well to all possible load vectors \mathbf{d} (our numerical tests suggest that it does) but in what other ways it can generalize. For example, one can imagine both the network structure and generation/flow constraints changing

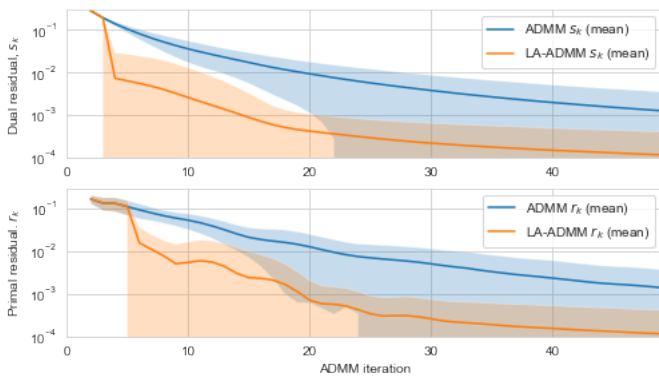


Fig. 3. Convergence of primal and dual residuals for ADMM (dark/blue) and LA-ADMM (light/orange) for the 300-bus test system with 5 partitions and 24 public branches. Solid lines indicate mean values and shaded regions indicate one standard deviation from the mean over 1000 test scenarios. Notice that the statistics match for the first 4 iterations before learned values are injected.

(for the former, if at a day ahead level, say, certain units were not planned to be operating; for the latter, due to, say weather or maintenance). Machine learning models do not readily generalize outside of the domain they were trained on, so these other ways the problem could change would require retraining, but that is not an insurmountable problem. We will also need to consider whether and how this method can be transferred to the true, nonlinear formulation.

Learning to Optimize: The specific technique we have invented for this work is part of a growing realization that fertile ground for application of machine learning is not to *replace* optimization but to *augment* it. In the present case we are using learning to accelerate online optimization of the same sized problem we learn from. In other cases this idea has been used to learn “heuristics” that allow for efficient solution of much *larger* problems than they were trained on [22]. (This is not out of the question here, but it is beyond the scope of the present paper.)

In any case, a benefit of such an approach that is hard to overemphasize is that the learned model is used *within* a generally convergent optimization scheme. With or without the learning, convergence provides a global, consistent, reliable measure of the quality of the solution. This helps alleviate a frequent and justified complaint that basing decisions on data-driven machine learning models is not appropriate in safety-critical systems.

REFERENCES

- [1] D. Bertsekas and J. Tsitsiklis, *Parallel and distributed computation: numerical methods*. Prentice hall Englewood Cliffs, NJ, 1989, vol. 23.
- [2] S. Boyd, N. Parikh, E. Chu, B. Peleato, and J. Eckstein, “Distributed optimization and statistical learning via the alternating direction method of multipliers,” *Foundations and Trends® in Machine learning*, vol. 3, no. 1, pp. 1–122, 2011.
- [3] T.-H. Chang, M. Hong, and X. Wang, “Multi-agent distributed optimization via inexact consensus admm,” *IEEE Transactions on Signal Processing*, vol. 63, no. 2, pp. 482–497, 2014.
- [4] R. Zhang and J. Kwok, “Asynchronous distributed admm for consensus optimization,” in *International Conference on Machine Learning*, 2014, pp. 1701–1709.

- [5] R. Nishihara, L. Lessard, B. Recht, A. Packard, and M. Jordan, “A general analysis of the convergence of admm,” in *International Conference on Machine Learning*, 2015, pp. 343–352.
- [6] G. França, D. Robinson, and R. Vidal, “Admm and accelerated admm as continuous dynamical systems,” *arXiv preprint arXiv:1805.06579*, 2018.
- [7] B. Chang, M. Chen, E. Haber, and E. Chi, “Antisymmetricrnn: A dynamical system view on recurrent neural networks,” *arXiv preprint arXiv:1902.09689*, 2019.
- [8] A. Kargarian, J. Mohammadi, J. Guo, S. Chakrabarti, M. Barati, G. Hug, S. Kar, and R. Baldick, “Toward distributed/decentralized dc optimal power flow implementation in future electric power systems,” *IEEE Transactions on Smart Grid*, vol. 9, no. 4, pp. 2574–2594, 2016.
- [9] D. Molzahn, F. Dörfler, H. Sandberg, S. Low, S. Chakrabarti, R. Baldick, and J. Lavaei, “A survey of distributed optimization and control algorithms for electric power systems,” *IEEE Transactions on Smart Grid*, vol. 8, no. 6, pp. 2941–2962, 2017.
- [10] T. Erseghe, “Distributed optimal power flow using admm,” *IEEE transactions on power systems*, vol. 29, no. 5, pp. 2370–2380, 2014.
- [11] Q. Peng and S. Low, “Distributed algorithm for optimal power flow on a radial network,” in *53rd IEEE Conference on decision and control*. IEEE, 2014, pp. 167–172.
- [12] P. Scott and S. Thiébaux, “Distributed multi-period optimal power flow for demand response in microgrids,” in *Proceedings of the 2015 ACM Sixth International Conference on Future Energy Systems*. ACM, 2015, pp. 17–26.
- [13] Y. Wang, L. Wu, and S. Wang, “A fully-decentralized consensus-based admm approach for dc-opf with demand response,” *IEEE Transactions on Smart Grid*, vol. 8, no. 6, pp. 2637–2647, 2016.
- [14] M. Ma, L. Fan, and Z. Miao, “Consensus admm and proximal admm for economic dispatch and ac opf with socp relaxation,” in *2016 North American Power Symposium (NAPS)*. IEEE, 2016, pp. 1–6.
- [15] Y. Zhang, E. Dall’Anese, and M. Hong, “Dynamic admm for real-time optimal power flow,” in *2017 IEEE Global Conference on Signal and Information Processing (GlobalSIP)*. IEEE, 2017, pp. 1085–1089.
- [16] Y. Zhang, M. Hong, E. Dall’Anese, S. Dhople, and Z. Xu, “Distributed controllers seeking ac optimal power flow solutions using admm,” *IEEE Transactions on Smart Grid*, vol. 9, no. 5, pp. 4525–4537, 2017.
- [17] S. Karagiannopoulos, P. Aristidou, and G. Hug, “Data-driven local control design for active distribution grids using off-line optimal power flow and machine learning techniques,” *IEEE Transactions on Smart Grid*, 2019.
- [18] R. Dobbe, O. Sondermeijer, D. Fridovich-Keil, D. Arnold, D. Callaway, and C. Tomlin, “Towards distributed energy services: Decentralizing optimal power flow with machine learning,” *IEEE Transactions on Smart Grid*, 2019.
- [19] A. Xavier, F. Qiu, and S. Ahmed, “Learning to solve large-scale security-constrained unit commitment problems,” *arXiv preprint arXiv:1902.01697*, 2019.
- [20] S. Babaeinejad-sarookolae, A. Birchfield, R. Christie, C. Coffrin, C. Demarco, R. Diao, M. Ferris, S. Fliscounakis, S. Greene, and R. Huang, “The power grid library for benchmarking ac optimal power flow algorithms,” *arXiv preprint arXiv:1908.02788*, 2019.
- [21] F. Parés, D. G. Gasulla, A. Vilalta, J. Moreno, E. Ayguadé, J. Labarta, U. Cortés, and T. Suzumura, “Fluid communities: a competitive, scalable and diverse community detection algorithm,” in *International Conference on Complex Networks and their Applications*. Springer, 2017, pp. 229–240.
- [22] E. Khalil, H. Dai, Y. Zhang, B. Dilkina, and L. Song, “Learning combinatorial optimization algorithms over graphs,” in *Advances in Neural Information Processing Systems*, 2017, pp. 6348–6358.